DOI: 10.1002/ejic.201000777

$BaAn^{IV}(PO_4)_2$ (An^{IV} = Th, Np) – A New Family of Layered Double Phosphates

Gilles Wallez,*[a] Damien Bregiroux,[a] Karin Popa,[b] Philippe E. Raison,[c] Christos Apostolidis,[c] Patric Lindqvist-Reis,[d] Rudy J. M. Konings,[c] and Aurelian F. Popa[e]

Keywords: Phosphates / Actinides / Solid-state structures / Layered compounds / Raman spectroscopy

$BaTh(PO_4)_2$ has been synthesized by a wet chemistry route and the new isotype $BaNp(PO_4)_2$ by solid-state reaction. Although the former has been the subject of several studies since the early 1980s, the crystal structures of both compounds are reported here for the first time. Rietveld analysis shows Ba layers alternating with $An(PO_4)_2$ slabs along the *a* axis. Although those compounds are isostructural to $RbEu(SO_4)_2$, these phosphates can be seen as modified yavapaiite derivatives with increased coordination numbers for Ba (XIV) and Th/Np (VIII). Raman and electron absorption spectra highlight the similarities and differences with chemically related compounds.

Introduction

$M^{II}M'^{IV}(PO_4)_2$ double phosphates have been intensively studied during the past two decades for applications including catalysts, ion conductors,[1] UV-emitting X-ray phosphors,[2] and also as potential host matrices for minor actinide immobilization.[3–4] Two main structural families can be distinguished, depending on the size of the cations. The yavapaiite family, from the archetype $KFe(SO_4)_2$ (monoclinic, *C*2/*m*),[5] comprises double phosphates made of layers of M^{II} cations in eight- or tenfold coordination substituted for K^{I}, alternating with dense slabs of $M'^{IV}O_6$ octahedra and $P^{V}O_4$ tetrahedra, replacing the $Fe^{III}O_6$ and $S^{VI}O_4$ units, respectively. It is typical of compounds in which the M^{II} and M'^{IV} cations are different enough in size to build specific environments, like in $BaZr(PO_4)_2$.[1,6] In contrast, the cheralite structure (formerly known as brabantite), isotypic with the $Ce^{III}PO_4$ monazite,[7] only hosts M^{II} and M'^{IV} cations similar in size with the light lanthanides, thus allowing them to occupy the same ninefold polyhedron in a disordered array. Because of the steric compatibility of tetravalent actinides with large divalent cations, most of the $M^{II}An^{IV}(PO_4)_2$ double phosphates discovered to date belong to this family.[8] In particular, $CaTh(PO_4)_2$ has attracted considerable interest for its ability to substitute tetravalent actinides (U^{IV},[9] Np^{IV},[10,11] and Pu^{IV} to a lesser extent[12]) by Th^{IV} while keeping the remarkable thermal[13,14] and chemical[15–23] durability of the monazite structure. For these reasons, monazite–cheralite ceramics figure among the most serious candidates for long-term immobilization of nuclear waste containing minor actinides.[24–28]

Two steric criteria of existence have been proposed by Podor et al. for cheralites:[29] the mean radius $[r(M^{II}) + r(M'^{IV})]/2$[30] must be in the range of those of the monazite-compatible lanthanides (La^{III} to Gd^{III}) and the critical $r(M^{II})/r(M'^{IV})$ ratio is between those of $PbTh(PO_4)_2$ (cheralite)[8] and $SrU(PO_4)_2$ (noncheralite).[31] In the global survey of the $M^{II}M'^{IV}(PO_4)_2$ double phosphates proposed in Figure 1, the domains corresponding to the different types have been plotted on the basis of structural data available in the literature. As opposed to the yavapaiite family, which comprises numerous chemical combinations, the cheralites appear limited by the narrowness of the steric criteria as well as by the rareness of large tetravalent cations. Indeed, all the known cheralites are actinide-based, but only calcium appears compatible with Th^{IV}, U^{IV}, Np^{IV}, and even Pu^{IV} in limited amounts, thus making it the only divalent cation eligible for forming a fully cheralite host matrix for minor actinides.

Figure 1 also evidences several actinide compounds that do not belong to any of these families. Although some of them have already been synthesized, nothing is known about their crystal chemistry, except for $SrNp(PO_4)_2$, which

[a] UPMC Univ. Paris 06, CNRS-UMR 7574, ENSCP-ParisTech, Laboratoire de Chimie de la Matière Condensée de Paris, 11 rue Pierre et Marie Curie, 75231 Paris Cedex 05, France
[b] Alexandru Ioan Cuza University, Department of Chemistry, 11 Carol I Blvd., 700506 Iasi, Romania
[c] European Commission, Joint Research Centre, Institute for Transuranium Elements, P. O. Box 2340, 76125 Karlsruhe, Germany
[d] Institute for Nuclear Waste Disposal, Karlsruhe Institute of Technology, Hermann-von-Helmholtz-Platz 1, 76344 Eggenstein-Leopoldshafen, Germany
[e] Institut des Matériaux Jean Rouxel (IMN), Université de Nantes, CNRS, 44322 Nantes, France

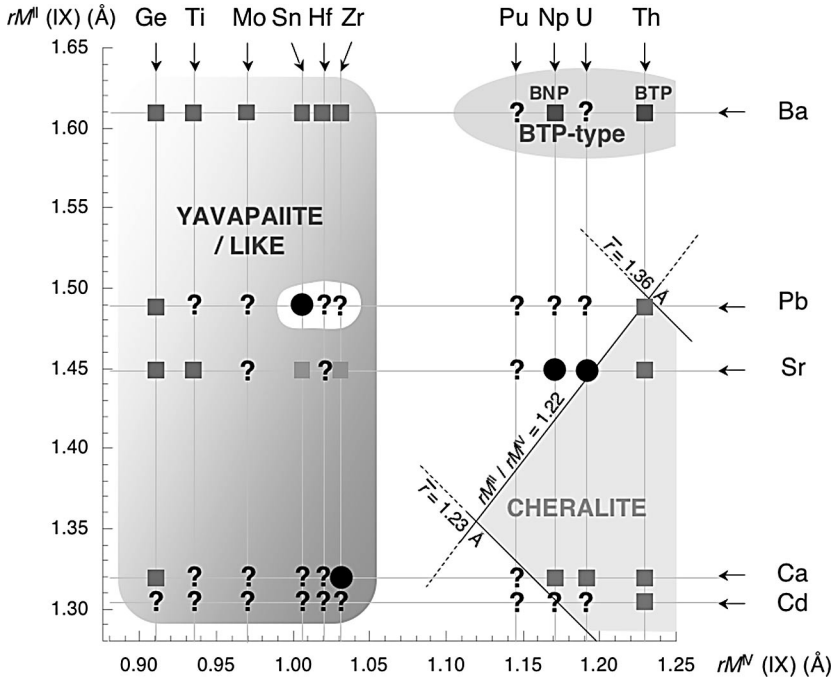

Figure 1. Presumed domains of existence of the main $M^{II}M'^{IV}(PO_4)_2$ types with radii of cations in ninefold coordination (from Shannon's cationic radii, r_c,[30] or extrapolated). The yavapaiite domain includes typical *C*2/*m* compounds and various derivatives. The unclassified compounds (black circles) belong to different families.

has been recently identified as an ordered derivative of cheralite.[32] Several authors[8,33–36] have reported the existence of $BaTh(PO_4)_2$, but its study and that of its derivatives is impeded by a complete lack of structural data. Even hypotheses concerning its crystal cell are divergent.

Considering the interest of this compound for both the fundamental chemistry of actinides and potential nuclear applications, we report here the synthesis and the first structural analysis of $BaTh(PO_4)_2$ (BTP) and the newly synthesized compound $BaNp(PO_4)_2$ (BNP).

Results and Discussion

The diffraction patterns of the two compounds are very similar. No isotype could be found among the known phosphates, but an excellent matching appeared between the diffraction patterns of BNP and $RbEu(SO_4)_2$,[37] consistent with the matching cationic radii between the two compounds.[8] The cell parameters and atomic positions were refined by Rietveld analysis.[38] The parameters and positions of the isotype were taken as a starting structural model (Figure 2). Anisotropic thermal factors were used for the heavy atoms (Ba, Th, Np), while those (isotropic) of the four independent oxygen atoms were treated as a single variable. Soft constraints were applied on the P–O distances. Main refinement parameters are reported in Table 1, atomic positions are presented in Table 2, and cation–anion distances are listed in Table 3. Ba and Th/Np occupy special positions, an inversion center and a twofold axis, respectively.

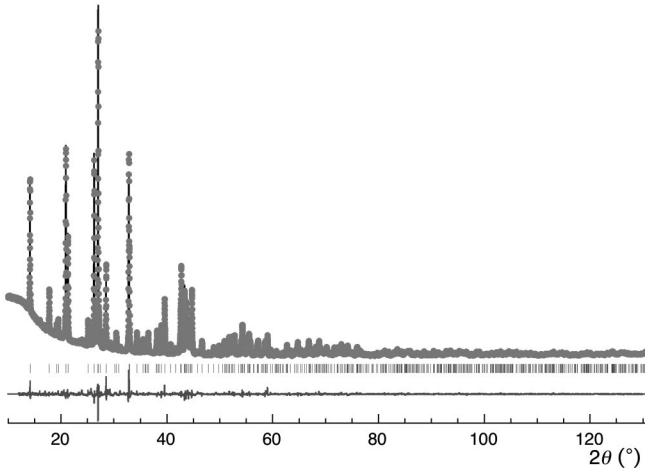

Figure 2. Final Rietveld plot for $BaTh(PO_4)_2$. Dots indicate observed intensities; the upper plot is calculated, and the lower plot shows the difference; the bars indicate the Bragg positions.

The BTP structure (Figure 3, left) is made of (100) layers of BaO_{14} polyhedra alternating with dense slabs of Th/NpO_8 square-based antiprisms (Figure 4) and PO_4 tetrahedra. The uncommon BaO_{14} units are distorted elongated hexagonal bipyramids (Figure 5) with short Ba–O3 bonds along the pseudo-senary axis. The BTP array is not unlike the stacking of Ba^{II} (001) layers and $Zr(PO_4)_2$ slabs in the two yavapaiite varieties of $BaZr(PO_4)_2$ [α with BaO_{10}[1] (Figure 3, right) or β with BaO_{12}[6] polyhedra].

To highlight the structural relationships, a would-be transition from yavapaiite to BTP could be thought of as

Table 1. Details of data collection, refinement conditions, and crystallographic data for $BaTh(PO_4)_2$ and $BaNp(PO_4)_2$.

	$BaTh(PO_4)_2$	$BaNp(PO_4)_2$
Temperature (K)	293	
Diffractometer	Siemens D8	
Scan mode	Bragg–Brentano	
Anode	Cu-K_α (40 kV, 40 mA)	
Monochromator	Ge (111)	
Detector	LynxEye	
Scan range (°)	$12.00 < 2\theta < 130.00$	
Step (°), total time (h)	0.0092, 36	
Reflections measured	634	655
Profile (model)	11 (pseudo-Voigt)	
Intensity depdt. params.	29	
Conventional reliability factors		
R_P	0.038	0.037
R_{wP}	0.055	0.052
$R_{exp.}$	0.021	0.041
χ^2	7.9	5.8
R_{Bragg}	0.029	0.036
Space group, system	$C2/c$ (15), monoclinic	
a (Å)	12.8053(7)	12.6937(6)
b (Å)	5.4400(3)	5.3641(3)
c (Å)	9.4636(5)	9.4139(5)
β (°)	102.247(3)	102.511(2)
Volume (Å^3)	644.2(1)	625.8(1)
Z	4	
Calcd. density (g cm^{-3})	4.79	4.98

Table 2. Atomic positions and thermal parameters for $BaTh(PO_4)_2$ and $BaNp(PO_4)_2$.

	x	y	z	B_{iso} (Å^2)[a]	Site
Ba	1/4	1/4	0	0.88(3)	4*c*
				0.87(2)	
Th/Np	0	0.1785(1)	1/4	0.50(1)	4*e*
		0.1754(1)		0.45(1)	
P	0.0919(1)	0.7351(3)	0.1111(1)	0.33(8)	8*f*
	0.0891(1)	0.7373(3)	0.1124(1)	0.54(6)	
O1	0.1571(5)	0.936(1)	0.2052(7)	1.0(1)	8*f*
	0.1526(3)	0.9469(8)	0.2058(6)	0.21(7)	
O2	0.1159(6)	0.4823(7)	0.1839(7)	id.	8*f*
	0.1064(4)	0.4781(6)	0.1833(6)		
O3	–0.0269(2)	0.805(1)	0.0858(7)	id.	8*f*
	–0.0296(2)	0.813(1)	0.0887(6)		
O4	0.1264(4)	0.724(1)	–0.0351(3)	id.	8*f*
	0.1212(3)	0.717(1)	–0.0357(3)		

[a] B_{eq} for Ba, Th, and Np.

follows: the two PO_4 tetrahedra turn into the slabs to share an edge with the tetravalent cation, increasing its coordination number from six to eight. Thus, the slab polyhedra increase their oxygen sharing (edges instead of vertices and faces instead of edges) with the interslab Ba^{II} cations. In turn, the Ba^{II} coordination number increases to fourteen. This also alternates shifts of the slabs perpendicular to the stacking axis and doubles the corresponding cell parameter. Actually, such a transition is likely to occur under high pressure. A BTP form could also change into an α or β yavapaiite at high temperature by the inverse process. Such phenomena have not yet been observed. In particular, the differential thermal analysis (DTA) did not show any phase transition for BTP between room temperature and 1250 °C.

Table 3. Selected interatomic distances (Å) for $BaTh(PO_4)_2$ and $BaNp(PO_4)_2$; bond valences are calculated by using Brown's parameters.[39]

		$BaTh(PO_4)_2$	$BaNp(PO_4)_2$
Ba–O1	2×	2.970(5)	2.972(5)
Ba–O1	2×	3.012(6)	2.994(5)
Ba–O2	2×	2.973(7)	3.027(6)
Ba–O2	2×	3.440(6)	3.462(5)
Ba–O3	2×	2.815(2)	2.761(3)
Ba–O4	2×	3.005(6)	2.972(5)
Ba–O4	2×	3.255(6)	3.273(5)
Bond valence sum		*1.90*	*1.96*
Th/Np–O1	2×	2.514(5)	2.404(4)
Th/Np–O2	2×	2.393(6)	2.285(5)
Th/Np–O3	2×	2.536(6)	2.447(6)
Th/Np–O4	2×	2.376(4)	2.329(3)
Bond valence sum		*3.74*	*3.91*
P–O1		1.541(5)	1.543(5)
P–O2		1.540(4)	1.537(4)
P–O3		1.537(3)	1.528(3)
P–O4		1.540(4)	1.539(4)
Bond valence sum		*4.76*	*4.80*

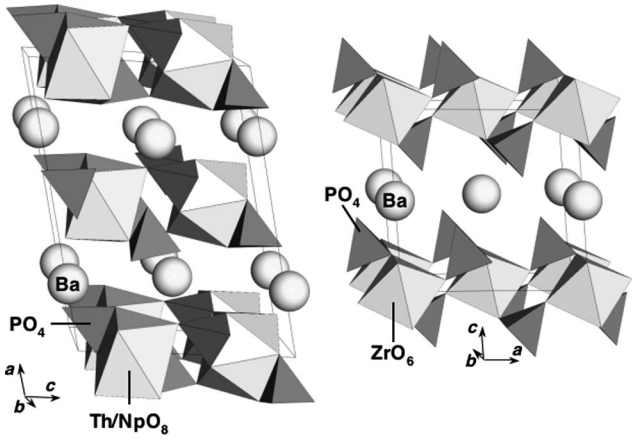

Figure 3. A comparison between the crystal structures of $BaTh(PO_4)_2$ (left) and α-$BaZr(PO_4)_2$ (right).

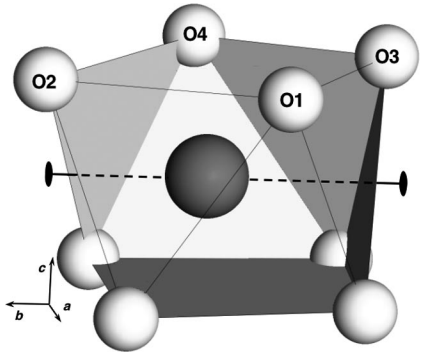

Figure 4. The ThO_8 square-based antiprism in BTP on the twofold axis.

Nonetheless, high-temperature and high-pressure experiments on BTP and $BaZr(PO_4)_2$ are in progress to check this hypothesis.

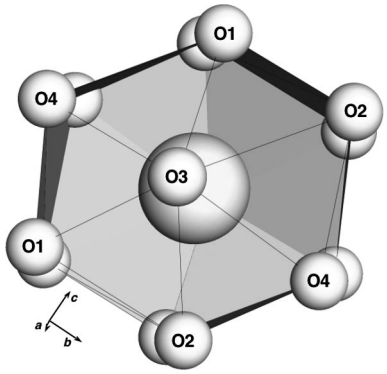

Figure 5. The centrosymmetric BaO_{14} polyhedron in BTP, observed along the pseudo-senary axis.

The high ratio between the ionic radii of the divalent and tetravalent cations in BTP and BNP results in the ordering of these cations into well-differentiated, fourteen- and eight-coordinate BaO_{14}/NpO_8 and BaO_{14}/ThO_8 entities, respectively. This makes these compounds clearly different from the cheralite-like structures $CaNp(PO_4)_2$ (CNP) and $SrNp(PO_4)_2$ (SNP), containing nine-, ten-, and eight-coordinate CaO_9/NpO_9 and SrO_{10}/NpO_8 entities, respectively.[6,32] These structural differences are also expressed in the IR and Raman spectra, which are sensitive to both the short- and long-range structures. The most obvious differences, however, are seen for the PO_4^{3-} stretching (ν_s, ν_{as}) and bending (δ_s, δ_{as}) bands, which differ in number, position, and splitting (Figure 6a,b). The fact that these bands are rather sharp is consistent with the relatively small tetrahedral distortion of the PO_4^{3-} ions, although the range of the P–O bond lengths is somewhat larger for BNP and SNP than for BTP (1.528–1.543, 1.542–1.564, and 1.537–1.541 Å, respectively). Consequently, the appreciably broader bands of CNP were attributed to the relatively distorted geometry of the phosphate ions (P–O 1.524–1.564 Å).[32] Although the IR and Raman spectra of BNP and SNP are quite different, their electronic absorption spectra are similar (Figure 7). This is reasonable, as the latter spectra monitor the Np^{4+} ($5f^3$) electronic transitions, which are modulated by the NpO_8 crystal fields.

In contrast to the XRD, infrared, and Raman data, which clearly show that BTP and BNP are different from the classical monazites, Orlova et al.[36] argued that BTP indeed is a classical monazite at room temperature but undergoes several phase transitions at higher temperatures between 650 and 1550 °C (in disagreement with our DTA data), whereas Montel et al.[35] suggested that BTP is a "double monazite" (doubled *a* axis). Considering the difficulties we met in obtaining BTP by the same (solid-state) route as these authors, a plausible origin for these discrepancies may be the different synthesis schemes used.

Since this new type of $BaAn(PO_4)_2$ phosphate is thermally stable for $An^{IV} = Th^{IV}$ (r_c = 1.19 Å, coord. VIII) and Np^{IV} (r_c = 1.12 Å, coord. VIII), it could likely host U^{IV} (r_c = 1.14 Å, coord. VIII); however, the synthesis of this compound should take place under argon (purity 4.6) because of the tendency of U^{IV} to oxidize into U^{VI} in air. Likewise, Pu^{IV} (r_c = 1.10 Å, coord. VIII) could also fit, provided that it does not reduce into Pu^{III}.

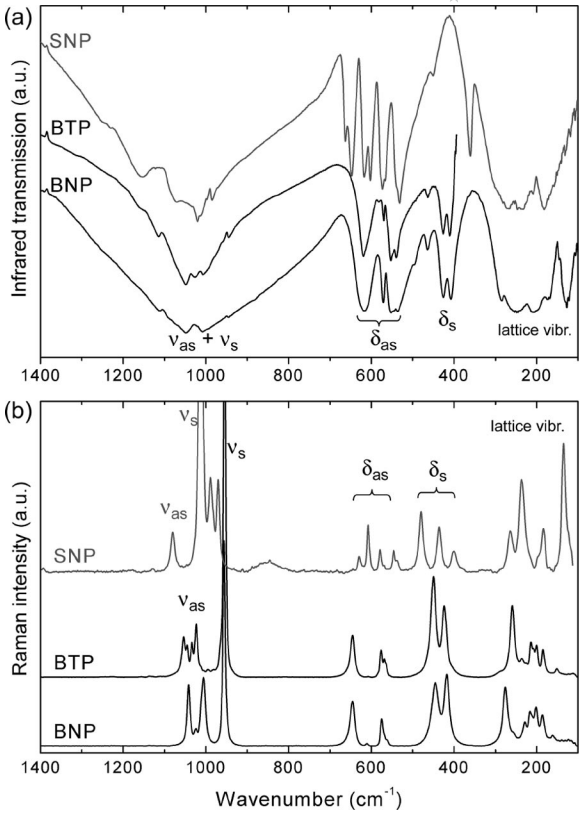

Figure 6. Room-temperature (a) IR and (b) Raman spectra of BNP, BTP, and SNP.

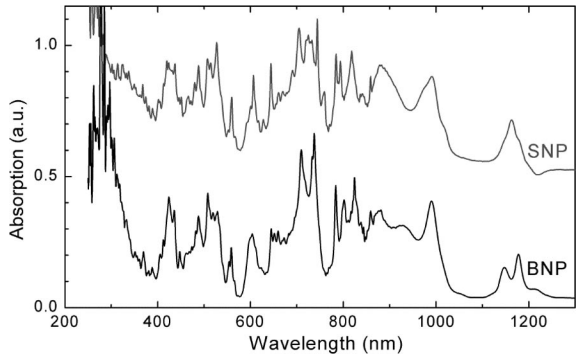

Figure 7. Room-temperature Np^{4+} ($5f^3$) electronic absorption spectra of SNP and BNP.

Recent studies concerning the thermal stability of $Th_2O(PO_4)_2$[40] and α-$Th_4(PO_4)_4(P_2O_7)$[41] showed that the sevenfold coordination is too small for Th^{IV}, whereas the ninefold coordination of cheralite is too big for Pu^{IV};[12,30] therefore, the eightfold square-based antiprism could be an ideal environment for the four actinide An^{IV} cations. For instance, a continuous solid solution between the BTP-type $BaAn^{IV}(PO_4)_2$ double phosphates could be of interest as a host matrix for the immobilization of uranium, plutonium, and minor actinides.

The classification proposed in Figure 1, despite being incomplete, suggests that there are several Sr and Pb compounds of different types in the intermediate zone between yavapaiites and cheralites. $SrNp(PO_4)_2$ shows differentiated SrO_{10} and NpO_8 polyhedra, which also build a layered array,[32] but it is more closely related to cheralite than to yavapaiite. Little is known about $SrU(PO_4)_2$, reported by Kitaev et al.[31] as a cheralite with "additional reflections of impurity phases" even after prolonged heating (800 °C, 400 h), but this compound could be related to $SrNp(PO_4)_2$. At last, recently discovered $SrSn(PO_4)_2$ (space group $C2/c$) appears as a distorted modification of yavapaiite,[42] while $SrZr(PO_4)_2$ ($P\bar{1}$) is considered by its discoverers as "probably isostructural with yavapaiite",[43] but in $PbSn(PO_4)_2$, the $6s^2$ lone pair affects strongly the Pb^{II} polyhedron, thus resulting in a unique structure.[44] Having in mind the almost identical ionic radii of the heaviest alkaline earth barium and radium,[30] one could predict that the radium-containing counterparts, $RaAn(PO_4)_2$, would adopt a similar layered structure as those of BTP and BNP.

Conclusions

The title compounds reveal a new family of double phosphates, clearly different from the cheralite to which BTP had been associated by previous authors, but rather related to yavapaiite. Further experiments will be carried out on the uranium and plutonium counterparts to ascertain the structural homogeneity of the $BaAn^{IV}(PO_4)_2$ family, which could be of interest for the synthesis of solid solutions such as host matrices for minor actinides. BTP and BNP also exhibit good thermal stability, which encourages the measurement of some thermochemical parameters associated to durability aspects, such as solubility. From a purely theoretical point of view, the search for possible phase transitions between BTP-type compounds and yavapaiites also appears as an interesting topic.

Experimental Section

Syntheses

We first tried to synthesize BTP by solid-state reaction, by heating ground mixtures of $Th_3(CO_3)_4$ (Prolabo, 99.5%), $BaCO_3$ (Prolabo, 99.5%), and $NH_4H_2PO_4$ (Sigma–Aldrich, 99%) at various temperatures between 1000 and 1300 °C. These powders showed significant residual diffraction peaks of ThO_2 and $Th_4(PO_4)_4(P_2O_7)$, both known for their high thermal stability. Therefore, an alternative wet process was explored by mixing aqueous solutions of $Th(NO_3)_4{\cdot}5H_2O$ (Sigma–Aldrich, 99%), $Ba(NO_3)_2$ (Prolabo, 99.5%), and $NH_4H_2PO_4$ (Sigma–Aldrich, 99%). The resulting gel was dehydrated at 120 °C in a stove, then heated slowly (10 °C h^{-1}) to 600 °C to avoid the loss of P_2O_5 during denitration. The sample was then annealed for 3×24 h at 1250 °C with intermediate grinding, which yielded a white powder with only faint ($I < 1.5\%\ I_{max}$) unidentified impurity diffraction peaks.

BNP was synthesized by a dry route in the specifically designed glove boxes for radioactive materials operating under nitrogen at the Institute for Transuranium Elements (Karlsruhe). Reactor grade $^{237}NpO_2$ (24.2 mg) was heated for 3 h at 886 °C under an atmosphere of air in order to eliminate surface water, carbon dioxide, etc. It was then mixed and ground with $BaCO_3$ (Merck, stoichiometric amount) and $(NH_4)_2HPO_4$ (Alfa Aesar, 5% excess) in an agate mortar, then heated in an alumina crucible for 10 h at 1108 °C under argon (purity 4.6, heating and cooling rates of 200 °C h^{-1}). After regrinding, a second thermal treatment was applied for 10 h at 1212 °C (same rate and atmosphere).

X-ray Diffraction: Acquisition parameters are reported in Table 1. To reduce the background, a silicon wafer was used as holder for the sample (about 50 mg).

Differential Thermal Analysis: DTA was performed in air with a Setaram 92 analyzer at a 300 °C h^{-1} heating rate.

IR Spectra: IR spectra of $BaNp(PO_4)_2$ (BNP) and $BaTh(PO_4)_2$ (BTP) were recorded with a Perkin–Elmer 2000 FTIR spectrophotometer at room temperature. The samples were diluted in KBr or polyethylene and pressed to tablets for recording mid- or far-infrared spectra, respectively.

Raman Spectra: Raman spectra of BNP and BTP powders were measured at room temperature by using a Bruker Senterra dispersive Raman microscope at 532 nm and 20 mW at a spectral resolution of 4 cm^{-1}. For each compound, five spectra were averaged and background correction was performed with the OPUS software from Bruker.

Further details on the crystal structure investigations may be obtained from the Fachinformationszentrum Karlsruhe, 76344 Eggenstein-Leopoldshafen, Germany (Fax: +49-7247-808-666; E-mail: crysdata@fiz-karlsruhe.de), on quoting the depository number CSD-421964 for BNP and CSD-421965 for BTP.

Acknowledgments

We acknowledge the financial support offered by the European Commission in the frame of the Actinet-I3 program (project JRP01). The authors would like to express their gratitude to D. Bouexière for the collection of the X-ray data. K. P. also thanks Prof. Vladimir Brandel for introducing him to this class of compounds.

[1] K. Fukuda, A. Moriyama, T. Iwata, *J. Solid State Chem.* **2005**, *178*, 2144–2151.
[2] C. R. Miao, C. C. Torardi, *J. Solid State Chem.* **2000**, *155*, 229–232.
[3] K. Popa, R. J. M. Konings, P. Boulet, D. Bouëxière, A. F. Popa, *Thermochim. Acta* **2005**, *436*, 51–55.
[4] K. Popa, H. Leiste, T. Wiss, R. J. M. Konings, *J. Radioanal. Nucl. Chem.* **2007**, *273*, 563–567.
[5] E. J. Graeber, A. Rosenzweig, *Am. Mineralog.* **1971**, *56*, 1917–1933.
[6] D. Bregiroux, K. Popa, R. Jardin, P. E. Raison, G. Wallez, M. Quarton, M. Brunelli, C. Ferrero, R. Caciuffo, *J. Solid State Chem.* **2009**, *182*, 1115–1120.
[7] G. W. Beall, L. A. Boatner, D. F. Mullica, W. O. Milligan, *J. Inorg. Nucl. Chem.* **1981**, *43*, 101–105.
[8] D. Rose, *Neues Jahrb. Mineral. Monatsh.* **1980**, *247*, 247–257.
[9] T. Muto, R. Meyrowitz, A. Pommer, T. Murano, *Am. Mineral.* **1959**, *44*, 633–650.
[10] A. Tabuteau, M. Pagès, J. Livet, C. Musikas, *J. Mater. Sci. Lett.* **1988**, *7*, 1315–1317.
[11] P. E. Raison, R. Jardin, D. Bouëxière, R. J. M. Konings, T. Geisler, C. C. Pavel, J. Rebizant, K. Popa, *Phys. Chem. Minerals* **2008**, *35*, 603–609.

[12] Bregiroux, R. Belin, P. Valenza, F. Audubert, D. Bernache-Assollant, *J. Nucl. Mater.* **2007**, *366*, 52–57.
[13] K. Popa, T. Shvareva, L. Mazeina, E. Colineau, F. Wastin, R. M. J. Konings, A. Navrotsky, *Am. Mineral.* **2008**, *93*, 1356–1362.
[14] R. Jardin, C. C. Pavel, P. E. Raison, D. Bouëxière, H. Santa-Cruz, R. J. M. Konings, K. Popa, *J. Nucl. Mater.* **2008**, *378*, 167–171.
[15] F. Poitrasson, S. Chenery, D. J. Bland, *Earth Planet. Sci. Lett.* **1996**, *145*, 79–96.
[16] O. Terra, N. Clavier, N. Dacheux, R. Podor, *New J. Chem.* **2003**, *27*, 957–967.
[17] F. Poitrasson, E. H. Oelkers, J. Schott, J.-M. Montel, *Geochim. Cosmochim. Acta* **2004**, *68*, 2207–2221.
[18] E. H. Oelkers, F. Poitrasson, *Chem. Geol.* **2002**, *191*, 73–87.
[19] N. Dacheux, N. Clavier, A.-C. Robisson, O. Terra, F. Audubert, J.-E. Lartigue, C. Guy, *C. R. Chim.* **2004**, *7*, 1141–1152.
[20] Z. S. Cetiner, S. A. Wood, C. H. Gammons, *Chem. Geol.* **2005**, *217*, 147–169.
[21] O. Terra, N. Dacheux, F. Audubert, R. Podor, *J. Nucl. Mater.* **2006**, *352*, 224–232.
[22] K. Popa, R. M. J. Konings, T. Wiss, H. Leiste, *J. Radioanal. Nucl. Chem.* **2007**, *273*, 563–567.
[23] E. du Fou de Kerdaniel, N. Clavier, O. Terra, N. Dacheux, R. Podor, *J. Nucl. Mater.* **2007**, *362*, 451–458.
[24] D. Bregiroux, S. Lucas, E. Champion, F. Audubert, D. Bernache-Assollant, *J. Eur. Ceram. Soc.* **2006**, *26*, 279–287.
[25] D. Bregiroux, F. Audubert, T. Charpentier, D. Sakellariou, D. Bernache-Assollant, *Solid State Sci.* **2007**, *9*, 432–439.
[26] D. Bregiroux, O. Terra, F. Audubert, N. Dacheux, V. Serin, R. Podor, D. Bernache-Assollant, *Inorg. Chem.* **2007**, *46*, 10372–10382.
[27] O. Terra, N. Dacheux, N. Clavier, R. Podor, F. Audubert, *J. Am. Ceram. Soc.* **2008**, *91*, 3673–3682.
[28] D. Bregiroux, F. Audubert, D. Bernache-Assollant, *Ceram. Int.* **2009**, *35*, 1115–1120.
[29] R. Podor, M. Cuney, *Am. Mineral.* **1997**, *82*, 765–771.
[30] R. D. Shannon, *Acta Crystallogr., Sect. A* **1976**, *32*, 751–767.
[31] D. B. Kitaev, Yu. F. Volkov, A. I. Orlova, *Radiochemistry* **2004**, *46*, 195–200.
[32] K. Popa, G. Wallez, P. E. Raison, D. Bregiroux, C. Apostolidis, P. Lindqvist-Reis, R. J. M. Konings, *Inorg. Chem.* **2010**, *49*, 6904–6908.
[33] Yu. F. Volkov, A. I. Orlova, *Sbornik Trudov FSUE "SSF RF RIAR"*, Dimitrograd (Russia), **1996**, pp. 25–42.
[34] V. Brandel, N. Dacheux, J. Rousselle, M. Genet, *R. Acad. Sci., Ser. IIc:. Chim.* **2002**, *5*, 599–606.
[35] J.-M. Montel, J.-L. Devidal, D. Avignant, *Chem. Geol.* **2002**, *191*, 89–104.
[36] A. I. Orlova, "Chemistry and Structural Chemistry of Anhydrous Tri- and Tetravalent Actinide Orthophosphates" in *Structural Chemistry of Inorganic Actinide Compounds* (Eds: S. V. Krivovichev, P. C. Burns, I. G. Tananaev), Elsevier B. V., Amsterdam, The Netherlands, **2007**.
[37] N. L. Sarukhanyan, L. D. Ishkakova, V. K. Trunov, *Kristallografiya* **1983**, *28*, 452–456.
[38] J. Rodriguez-Carvajal, *FULLPROF.2k: Rietveld, Profile Matching and Integrated Intensity Refinement of X-ray and Neutron Data*, V 1.9c, Laboratoire Léon Brillouin, CEA, Saclay, France, **2001**.
[39] I. D. Brown, **2009**. http://www.ccp14.ac.uk/ccp/web-mirrors/i_d_brown/bond_valence_param/bvparm2006.cif.
[40] N. Dacheux, N. Clavier, G. Wallez, M. Quarton, *Solid State Sci.* **2007**, *9*, 619–627.
[41] G. Wallez, N. Clavier, N. Dacheux, M. Quarton, W. van Beek, *J. Solid State Chem.* **2006**, *179*, 3007–3016.
[42] K. Fukuda, A. Moriyama, S. Hashimoto, *J. Solid State Chem.* **2004**, *177*, 3514–3521.
[43] D. Zhao, H. Zhang, Z. Xie, W. L. Zhang, S. L. Yang, W. D. Cheng, *Dalton Trans.* **2009**, 5310–5318.
[44] E. Morin, G. Wallez, S. Jaulmes, J.-C. Couturier, M. Quarton, *J. Solid State Chem.* **1998**, *136*, 283–288

Received: July 16, 2010
Published Online: December 2, 2010

